13.4

The influence of accelerating voltage fluctuations on the synchronization bandwidth of a megawatt-class gyrotron

© R.M. Rozental, A.P. Fokin

Institute of Applied Physics, Russian Academy of Sciences, Nizhny Novgorod, Russia
E-mail: rrz@ipfran.ru

Received November 9, 2023
Revised February 8, 2024
Accepted February 14, 2024

For a 170 GHz gyrotron with the output power level of 2 MW, calculations were performed in the framework of the particle-in-cells method. Calculations were carried out according to the equivalent axially symmetric gyrotron model with taking into account electron energy fluctuations induced by fluctuations in the output voltage of the high-voltage power supply. The output radiation spectrum width calculated in this way (about 1 MHz) complies with the experimental data. With the aid of this model we have shown that, in the problem of gyrotron locking by an external signal, accounting for voltage fluctuations leads to a decrease in the design locking bandwidth: by 13% at the external signal power of 20 kW and by 27% at that of 5 kW.

Keywords: gyrotron, frequency locking by an external signal, millimeter-wave radiation.

DOI: 10.61011/TPL.2024.05.58427.19797

One of the key elements of controlled thermonuclear fusion facilities based on microwave heating of plasma are gyrotrons capable of providing continuous generation of the millimeter-wave megawatt-power radiation [1,2]. Again, one of the important tasks in creating such gyrotrons is stabilizing their oscillation frequency. At present, two approaches to solving this problem are being developed. One of them is based on creating circuits for automatic frequency control by varying the electron beam parameters [3]. Another approach is based on using an external oscillator ensuring locking of high-power gyrotron oscillations [4–7]. Here the role of external oscillator is played by a lower-power gyrotron equipped with a frequency-stabilization circuit [8].

This paper presents calculations of a 170 GHz gyrotron operating in the regime of subjecting it to an external signal. The main distinction of this study from previous ones is accounting for the finite gyrotron spectrum width which is determined by the presence of fluctuations in the electron beam energy. Notice that in recent work [9] there was considered the influence of a number of beam characteristics inherent to a real experiment (initial scattering of electron transverse velocities, final beam thickness, displacement of the beam injection axis relative to the cavity axis) on the gyrotron efficiency in the autonomous regime and in the regime of locking by the external signal. However, the problem of the effect of these characteristics on the locking bandwidth was not considered.

Consider a 170 GHz gyrotron powered by an electron beam 100 keV in energy and 50 A in current, in which there is excited operating mode $TE_{m,p}$ with azimuthal index $m = 28$ and radial index $p = 12$ [10]. For high-voltage gyrotron power supplies, the required magnitude of accelerating voltage fluctuations are being set at no more than 1% [11,12]; however, in practice those fluctuations are tried to be restricted to several tenths of a percent [13]. Such fluctuations are known to give rise to fluctuations in the gyrotron oscillation frequency [14,15], which are observed experimentally. Figure 1, *a* presents the experimentally measured spectrum of a high-power gyrotron operating at the frequency of $f_0 = 169.907$ GHz. As shown, the spectrum characteristic width is about 1 MHz.

The gyrotron was modeled by the particle-in-cells method using code KARAT [16]. To decrease the calculation

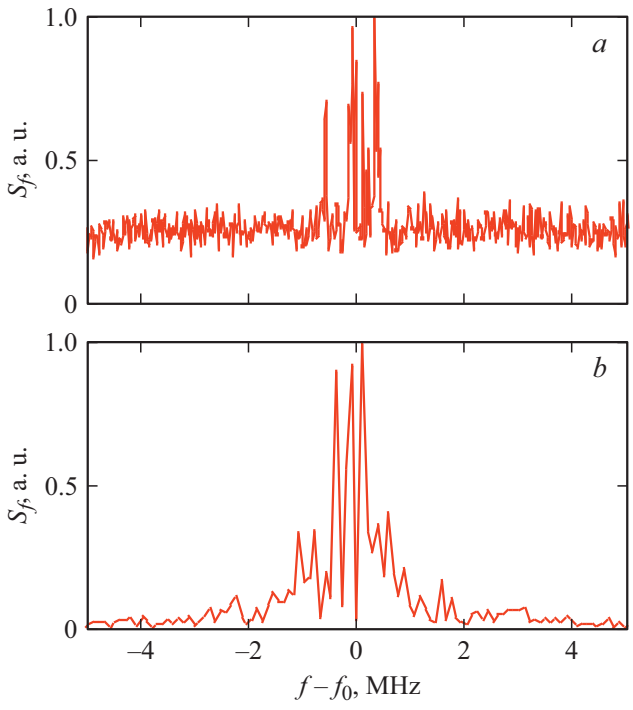

Figure 1. Experimentally measured (*a*) and model (*b*) spectra of the gyrotron output radiation.

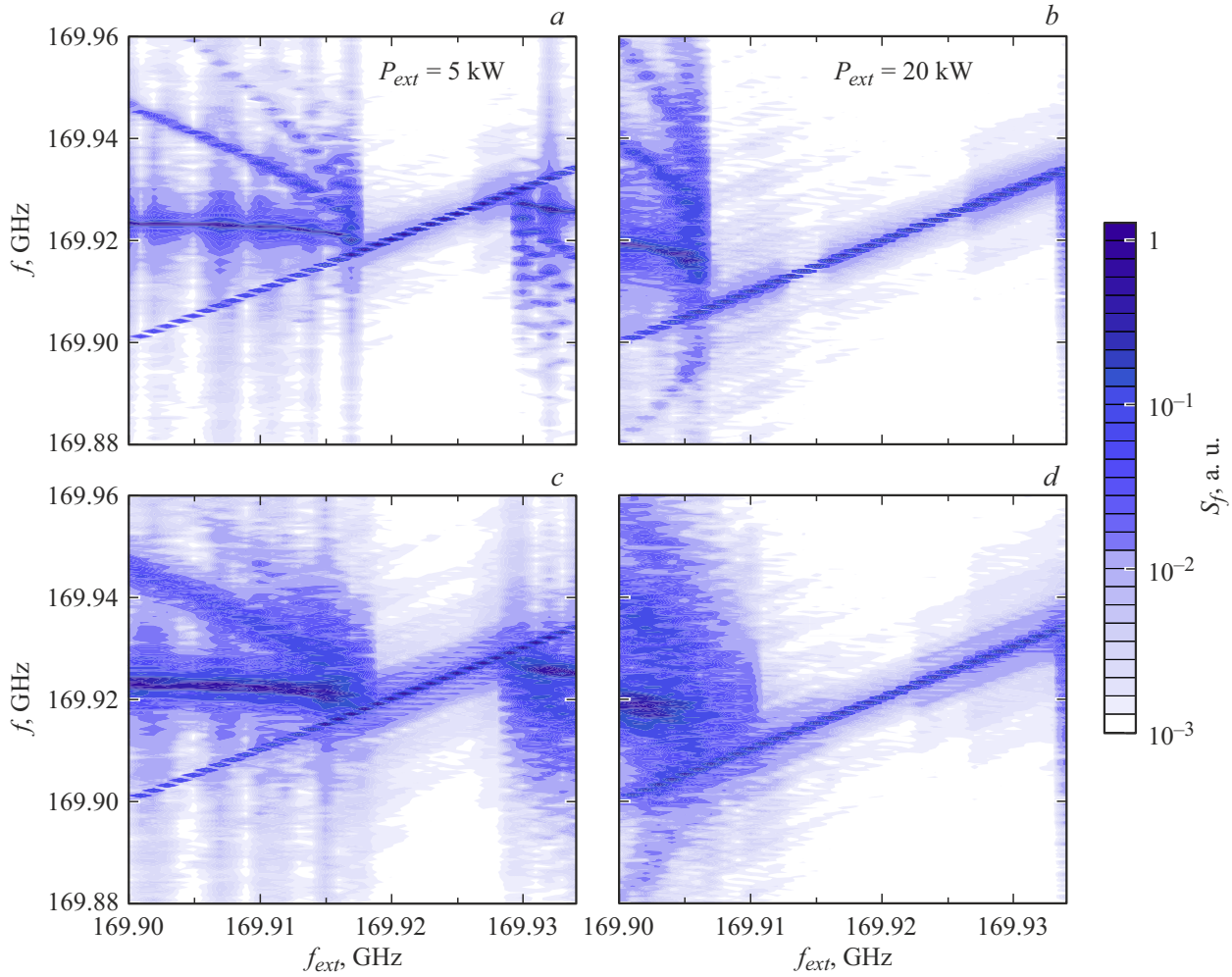

Figure 2. Gyrotron spectrograms in the absence of accelerating voltage fluctuations (a, b) and in their presence (c, d). The left panels present the data at the external signal power $P_{ext} = 5$ kW, the right ones present those for $P_{ext} = 20$ kW.

time, the three-dimensional problem of modeling a gyrotron with an asymmetric operating mode was reduced to the 2.5-dimensional one [17]. For this purpose, there was selected an equivalent axisymmetric mode having a close coefficient of coupling with the electron beam:

$$G_{mp} = \frac{J_{m-1}^2(\nu_{mp} R_{beam}/R_0)}{J_m^2(\nu_{mp})(\nu_{mp}^2 - m^2)}, \qquad (1)$$

where ν_{mp} is the p-th root of equation $J'_m(\nu) = 0$, $J_m(x)$ is the Bessel function, R_0, R_{beam} are the radii of the uniform cavity section and electron beam injection. As for the gyrotron under study, the most suitable mode is $TE_{M,P}$ with azimuthal index $M = 0$ and radial index $P = 13$, whose difference in the coupling coefficients is about 4%. In the equivalent task, the cavity profile is recalculated as

$$R_{0,13}(z) = \frac{\nu_{0,13}}{\nu_{28,12}} R_{28,12}(z), \qquad (2)$$

where $R_{0,13}(z)$, $R_{28,12}(z)$ are the cavity radius dependences on the longitudinal coordinate in the equivalent and initial gyrotrons, respectively. Variation in the cavity profile is followed by variation in the operating oscillation Q-factor. In addition, to accelerate the calculation, the electrodynamic system boundaries were assumed to be perfectly conductive and, hence, ohmic losses were ignored in modeling. However, since for the gyrotron under study the ohmic Q-factor significantly exceeds the diffraction Q-factor under the above-described approximations, the final difference in Q-factors is only about 1.5% and does not significantly affect the final calculation result.

In modeling, a helical electron beam with a pitch factor (ratio between the transverse and longitudinal electron velocities) of 1.2 excited the gyrotron cavity at the $TE_{0,13}$ mode and, after the end of interaction, was deposited on the electrodynamic system wall in the range of the guiding magnetic field decay. The maximum design oscillation power of the gyrotron was 2.1 MW. The oscillation frequency was $f_0 \approx 169.93$ GHz. The modeling was performed at the times of about 5 μs. In calculations, the electron beam initial energy was varied randomly every 100 ns in the range of ± 0.2 keV; due to this, the gyrotron radiation

spectrum width was, as in the experiment, about 1 MHz (Fig. 1, *b*). When the gyrotron was supplied with an external signal with frequency $f_{ext} = f_0$ and power $P_{ext} \geqslant 5$ kW, the radiation spectrum became practically indistinguishable from the spectrum in the gyrotron free of fluctuations in the initial energy of particles [17]. The spectrum width was thereat about 0.2 MHz which is equal to the reverse duration of the case under calculation; this is clearly shown in Figs. 2, *c*, *d* where spectrograms of the gyrotron output radiation are presented.

Of significant practical interest is studying the gyrotron dynamics under the conditions of detuning of the external frequency f_{ext} from oscillation eigenfrequency f_0. This is first of all associated with insufficient manufacturing precision of the gyrotron cavity, which may result in the difference between oscillation eigenfrequencies of the high-power gyrotron and external source, and also with the necessity to change the high-power gyrotron oscillation regime during operation. Remind that, in the ideal system, in the range of f_{ext}variation there is a locking region where the oscillation frequency is equal to that of the external signal. Beyond this region, the multifrequency oscillation regime arises. The distance between spectral components changes in this case from zero at the locking region boundary to $|f_{ext} - f_0|$ at the infinitely long distance from the boundary [18,19]. In the simplest case, the locking region width is proportional to the external impact magnitude and inversely proportional to the cavity Q-factor.

To determine the width of the region of gyrotron locking by the external signal, the gyrotron operating point (electron beam current and average energy, guiding magnetic field magnitude) was fixed, and the external signal frequency was varied in the range of 169.9–169.935 GHz. Figs. 2, *a*, *b* demonstrate spectrograms of the gyrotron output radiation upon injection of a monoenergetic helical electron beam. In this case, the locking region boundaries are $f_{ext} = 169.918–169.929$ GHz at the external signal power of 5 kW (Fig. 2, *a*) and $f_{ext} = 169.907–169.933$ GHz at 20 kW (Fig. 2, *b*). Beyond the locking region, the system turns to the regime of multifrequency oscillation. Figs. 2, *c*, *d* present spectrograms of the output radiation in the presence of the beam energy fluctuations. One can see that, when the external signal power is 5 kW, the locking region boundaries shift to $f_{ext} = 169.919–169.928$ GHz (Fig. 2, *c*), i. e. the locking bandwidth decreases from 11 to 8 MHz. When the external signal power is 20 kW, the locking region boundaries shift to $f_{ext} = 169.910–169.933$ GHz (Fig. 2, *d*), i. e. the locking bandwidth decreases from 26 to 23 MHz. In relative units, the locking bandwidth decrease for the external signal of 5 kW is about 27%, while that for the external signal of 20 kW is about 13%.

Thus, we can conclude that accelerating voltage fluctuations have a noticeable effect on the synchronization processes, especially in case of low external signal powers; hence, it is reasonable to take this effect into account in designing high-power gyrotrons to be operated in the regime of locking by the external signal.

In conclusion, notice that the proposed modeling method may also be used for higher-frequency gyrotrons currently being developed for the next-generation thermonuclear fusion facility (project DEMO) [20]. Such gyrotrons will need selection of a suitable equivalent model, however, the modeling approach itself will, obviously, remain the same. In addition, a similar model may be used in the problem when selective excitation of operating-mode oscillations gets realized only in the presence of an external locking source [21].

Acknowledgements

The authors express their gratitude to A.N. Kuftin and E.M. Tai for providing experimental data and participating in discussions.

Funding

The study was supported by the Russian Science Foundation (project № 19-79-30071).

Conflict of interests

The authors declare that they have no conflict of interests.

References

[1] M.K.A. Thumm, G.G. Denisov, K. Sakamoto, M.Q. Tran, Nucl. Fusion, **59** (7), 073001 (2019). DOI: 10.1088/1741-4326/ab2005

[2] A.G. Litvak, G.G. Denisov, M.Yu. Glyavin, IEEE J. Microwaves, **1** (1), 260 (2021). DOI: 10.1109/JMW.2020.3030917

[3] L. Krier, K.A. Avramidis, H. Braune, G. Gantenbein, S. Illy, J. Jelonnek, H.P. Laqua, S. Marsen, D. Moseev, F. Noke, T. Ruess, T. Stange, M. Thumm, R.C. Wolf, W7-X Team, Fusion Eng. Des., **192**, 113828 (2023). DOI: 10.1016/j.fusengdes.2023.113828

[4] V.L. Bakunin, G.G. Denisov, Yu.V. Novozhilova, Tech. Phys. Lett., **40** (5), 382 (2014). DOI: 10.1134/S1063785014050034.

[5] K.A. Yakunina, A.P. Kuznetsov, N.M. Ryskin, Phys. Plasmas, **22** (11), 113107 (2015). DOI: 10.1063/1.4935847

[6] I.V. Zotova, N.S. Ginzburg, G.G. Denisov, R.M. Rozental', A.S. Sergeev, Radiophys. Quantum Electron., **58** (9), 684 (2016). DOI: 10.1007/s11141-016-9640-7.

[7] G. Denisov, A. Kuftin, V. Manuilov, A. Chirkov, L. Popov, V. Zapevalov, A. Zuev, A. Sedov, I. Zheleznov, M. Glyavin, Nucl. Fusion, **62** (3), 036020 (2022). DOI: 10.1088/1741-4326/ac4946

[8] A.N. Kuftin, G.G. Denisov, A.V. Chirkov, M.Yu. Shmelev, V.I. Belousov, A.A. Ananichev, B.Z. Movshevich, I.V. Zotova, M.Yu. Glyavin, IEEE Electron Dev. Lett., **44** (9), 1563 (2023). DOI: 10.1109/LED.2023.3294755

[9] V.L. Bakunin, M.Yu. Glyavin, G.G. Denisov, Yu.V. Novozhilova, J. Infrared Millim. Terahertz Waves, **44** (7-8), 516 (2023). DOI: 10.1007/s10762-023-00930-5

[10] V.E. Myasnikov, M.V. Agapova, A.N. Kuftin, V.E. Zapevalov, G.G. Denisov, V.I. Ilin, L.M. Belnova, A.V. Chirkov, A.P. Gnedenkov, A.G. Litvak, V.I. Malygin, in *2013 38th Int. Conf. on infrared, millimeter, and terahertz waves (IRMMW-THz)* (IEEE, 2013), p. 1-2. DOI: 10.1109/IRMMW-THz.2013.6665557
[11] D. Fasel, F. Albajar, T. Bonicelli, A. Perez, L. Rinaldi, U. Siravo, L. Sita, G. Taddia, Fusion Eng. Des., **86** (6-8), 872 (2011). DOI: 10.1016/j.fusengdes.2011.02.017
[12] S.X. Ma, M. Zhang, L.L. Xia, Z. Zeng, X.L. Zhang, C.L. Wang, K.X. Yu, IEEE Trans. Plasma Sci., **42** (3), 656 (2014). DOI: 10.1109/TPS.2014.2300506
[13] G.G. Denisov, V.I. Malygin, A.I. Tsvetkov, A.G. Eremeev, M.Yu. Shmelev, V.I. Belousov, I.S. Baber, N.I. Karpov, I.I. Leonov, E.A. Kopelovich, M.M. Troitskiy, M.V. Kuznetsov, I.A. Varygin, K.A. Zhurin, B.Z. Movshevich, A.V. Chirkov, M.Yu. Glyavin, E.M. Tai, E.A. Soluyanova, M.I. Bakulin, I.N. Roy, I.O. Anashkin, P.P. Khvostenko, N.A. Kirneva, Radiophys. Quantum Electron., **63** (5-6), 332 (2020). DOI: 10.1007/s11141-021-10058-y.
[14] V.S. Ergakov, A.A. Shaposhnikov, Radiophys. Quantum Electron., **20** (8), 840 (1977). DOI: 10.1007/BF01038794.
[15] O. Dumbrajs, G.S. Nusinovich, Phys. Plasmas, **4** (5), 1413 (1997). DOI: 10.1063/1.872345
[16] V.P. Tarakanov, EPJ Web Conf., **149**, 04024 (2017). DOI: 10.1051/epjconf/20171490
[17] R.M. Rozental, E.M. Tai, V.P. Tarakanov, A.P. Fokin, Radiophys. Quantum Electron., **65** (5-6), 384 (2022). DOI: 10.1007/s11141-023-10221-7.
[18] R. Adler, Proc. IRE, **34** (6), 351 (1946). DOI: 10.1109/JRPROC.1946.229930
[19] V.L. Bakunin, G.G. Denisov, Yu.V. Novozhilova, Radiophys. Quantum Electron., **62** (7), 490 (2019). DOI: 10.1007/s11141-020-09995-x.
[20] G.G. Denisov, M.Yu. Glyavin, A.P. Fokin, A.N. Kuftin, A.I. Tsvetkov, A.S. Sedov, E.A. Soluyanova, M.I. Bakulin, E.V. Sokolov, E.M. Tai, M.V. Morozkin, M.D. Proyavin, V.E. Zapevalov, Rev. Sci. Instrum., **89** (8), 084702 (2018). DOI: 10.1063/1.5040242
[21] V.L. Bakunin, G.G. Denisov, Yu.V. Novozhilova, IEEE Electron Dev. Lett., **41** (5), 777 (2020). DOI: 10.1109/LED.2020.2980218

Translated by EgoTranslating